

Supporting Information

Ryu et al. 10.1073/pnas.1324301111

SI Materials and Methods

Bioinformatics. Multiple sequence alignments were generated using MUSCLE (1). Secondary structure predictions were performed using the Jpred3 server (2). Modeling of 3D structures was done using Swiss Model (3) project mode and a beta version of the next Swiss Model (4).

Protein Overexpression and Purification. The IlaC proteins were purified as C-terminal His₆-tagged fusions using Ni-affinity (Ni-NTA) chromatography according to specifications of the manufacturer (Novagen). Protein purification was performed under green light. The overnight cultures of *Escherichia coli* BL21 [DE3] expressing the IlaC::His₆ proteins were grown in LB supplemented with appropriate antibiotics at room temperature to A₆₀₀ 0.7. Protein expression was induced with IPTG at a final concentration of 0.5 mM, and the cultures were incubated with shaking at 250 rpm at 18 °C for an additional 20 h. Bacteria were collected by centrifugation at 4,000 × g for 10 min, washed, and resuspended in the binding buffer [50 mM sodium phosphate (pH 8.0), 300 mM NaCl] supplemented with 0.2 mM phenylmethylsulfonyl fluoride and 10 mM imidazole. Cells were disrupted using a French pressure cell, and cell debris was removed by centrifugation at 35,000 × g for 45 min at 4 °C. Three milliliters (bed volume) of Ni-NTA resin (Novagen) preequilibrated with

the binding buffer was added to the soluble cell extract derived from a 1-L culture and agitated for 1 h at 4 °C. The mix was loaded onto a column, and the resin was washed with 200 mL of column binding buffer. Fractions were eluted with 12 mL of binding buffer containing 250 mM imidazole. The proteins were either used immediately or stored at –80 °C in 20% vol/vol glycerol (final concentration). Protein concentrations were measured using a Bradford protein assay kit (Bio-Rad) with BSA as the protein standard. Proteins were analyzed using SDS/PAGE.

Adenylate Cyclase Assays. A standard reaction mixture (300 μL) contained 5 μM enzyme in the assay buffer [50 mM Tris-HCl (pH 8.0), 10% glycerol, 10 mM MgCl₂, 0.5 mM EDTA]. The protein was irradiated with either dim green light or far-red light emitted from a 1-W (700 nm) light-emitting diode (LED) at the approximate irradiance of 0.2 mW cm^{–2}. The reaction was started by the addition of ATP. Aliquots (50 μL) were withdrawn at different time points and immediately boiled for 5 min. The precipitated protein was removed by centrifugation at 15,000 × g for 5 min. The supernatant was filtered through a 0.22-μm pore size filter (MicroSolv). cAMP levels were analyzed by reversed-phase HPLC (HPLC) as described earlier (5).

1. Edgar RC (2004) MUSCLE: Multiple sequence alignment with high accuracy and high throughput. *Nucleic Acids Res* 32(5):1792–1797.
2. Arnold K, Bordoli L, Kopp J, Schwede T (2006) The SWISS-MODEL workspace: A web-based environment for protein structure homology modelling. *Bioinformatics* 22(2):195–201.
3. Cole C, Barber JD, Barton GJ (2008) The Jpred 3 secondary structure prediction server. *Nucleic Acids Res* 36(Web Server issue):W197–201.
4. Benkert P, Biasini M, Schwede T (2011) Toward the estimation of the absolute quality of individual protein structure models. *Bioinformatics* 27(3):343–350.
5. Ryjenkov DA, Tarutina M, Moskvina OV, Gomelsky M (2005) Cyclic diguanylate is a ubiquitous signaling molecule in bacteria: Insights into biochemistry of the GGDEF protein domain. *J Bacteriol* 187(5):1792–1798.

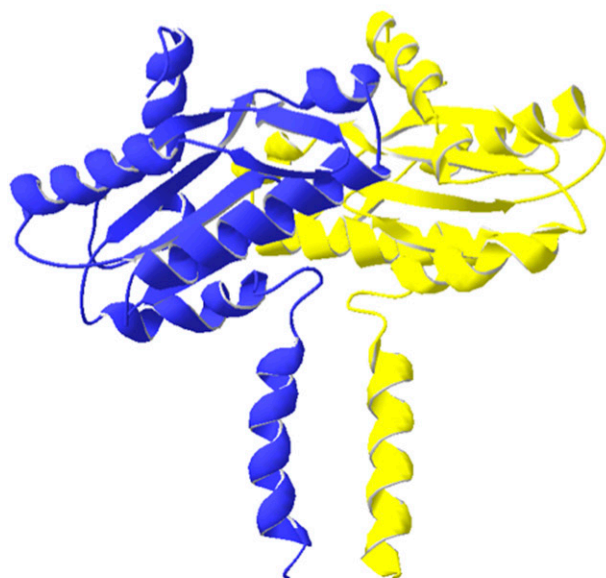
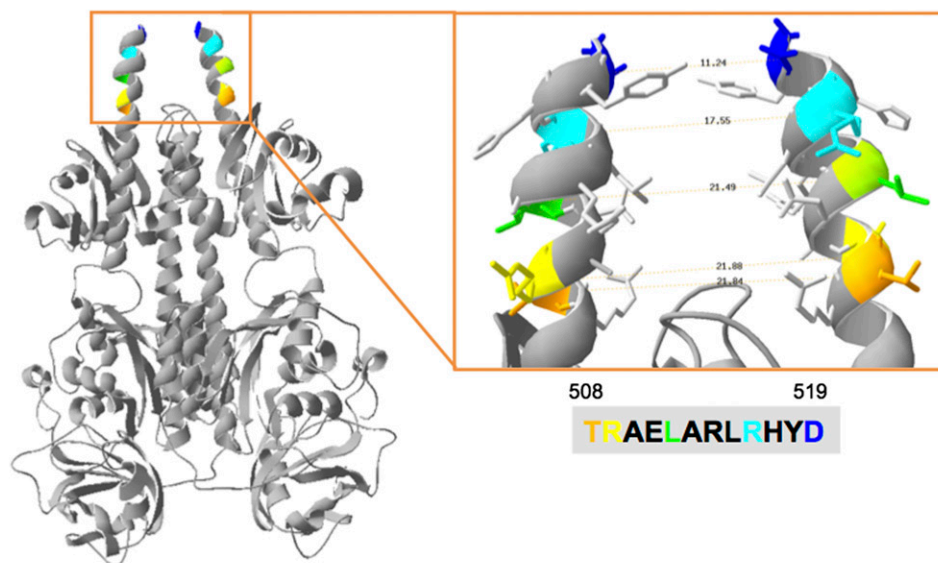
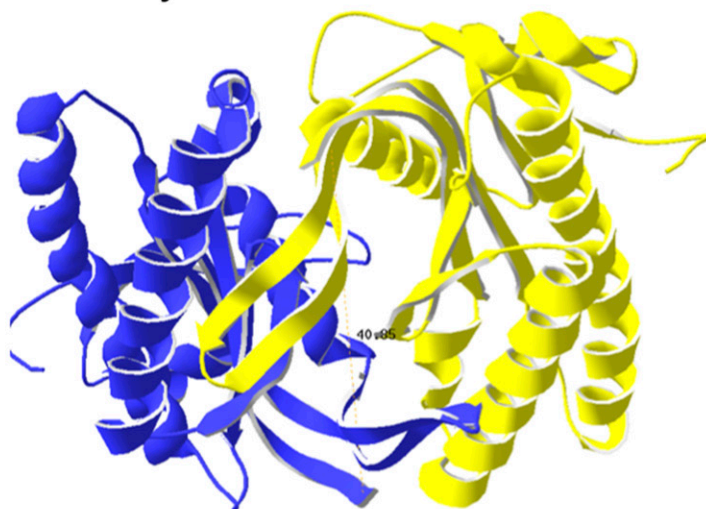
BphG GGDEF homodimer**CyaB1 AC homodimer****BphG PAS-GAF-PHY homodimer**

Fig. S1. Structural models of BphG and the adenylate cyclase (AC) domain of CyaB1. The parallel dimer of the bacteriophytochrome photosensory domains (PAS–GAF–PHY, where PAS, GAF, and PHY are protein domain names) was constructed using two Protein Data Bank structures, combined in several steps. First, a parallel dimer was built using 3C2W (1) as a template. Second, a monomer based on using 4GW9 (2) as a template was built to model the extended C-terminal α -helix from the PHY domain. To extend the aligned region of the C-terminal α -helix so that it could be modeled, the sequence was anchored to 4GW9 by including the anchoring sequence fragment “YEQFSSQVHASMQPVLITDAEGRIL” from 4GW9. This allowed us to model the region that is critical for estimating the distance between the extended α -helices that lead to the output domains despite low sequence identity. Third, the extended monomers were trimmed of the anchoring segment and superimposed onto the parallel dimer. Finally, the parallel dimer was modeled based on the combined template from the first three steps. This multistep modeling procedure was required to model the region important for estimating the distance between the extended α -helices that connect PHY and AC domains. Steps 1, 3, and 4 were modeled using Swiss Model project mode, whereas the second step was built using the beta version of the next Swiss Model (3). The dimer of GGDEF was constructed using 4H54 (4) as a template. The dimer of AC domains was constructed using 3R5G (5) as a template. Both dimers of the output domains were built using the beta version of Swiss Model (3). Shown are models of the dimers of the BphG GGDEF domains, CyaB1 AC domains, and the BphG PAS–GAF–PHY modules. The approximate distances between α -helical residues and between the N-terminal residues of the AC domain are shown (in angstroms). Note that in the photoactivated IlaC proteins, the AC domains are fused to the residues located approximately on the same phase of the α -helix that connects the PHY and AC domains, i.e., IlaC25 (Thr508, dark-yellow), IlaC22 (Arg509, light-yellow), IlaC17 (Leu512, green), and IlaC29 (Arg516, cyan).

1. Yang X, Kuk J, Moffat K (2008) Crystal structure of *Pseudomonas aeruginosa* bacteriophytochrome: Photoconversion and signal transduction. *Proc Natl Acad Sci USA* 105(38):14715–14720.
2. Bellini D, Papiz MZ (2012) Structure of a bacteriophytochrome and light-stimulated protomer swapping with a gene repressor. *Structure* 20(8):1436–1446.

3. Arnold K, Bordoli L, Kopp J, Schwede T (2006) The SWISS-MODEL workspace: A web-based environment for protein structure homology modelling. *Bioinformatics* 22(2):195–201.
4. Zähringer F, Lacanna E, Jenal U, Schirmer T, Boehm A (2013) Structure and signaling mechanism of a zinc-sensory diguanylate cyclase. *Structure* 21(7):1149–1157.
5. Topal H, et al. (2012) Crystal structure and regulation mechanisms of the CyaB adenylyl cyclase from the human pathogen *Pseudomonas aeruginosa*. *J Mol Biol* 416(2):271–286.

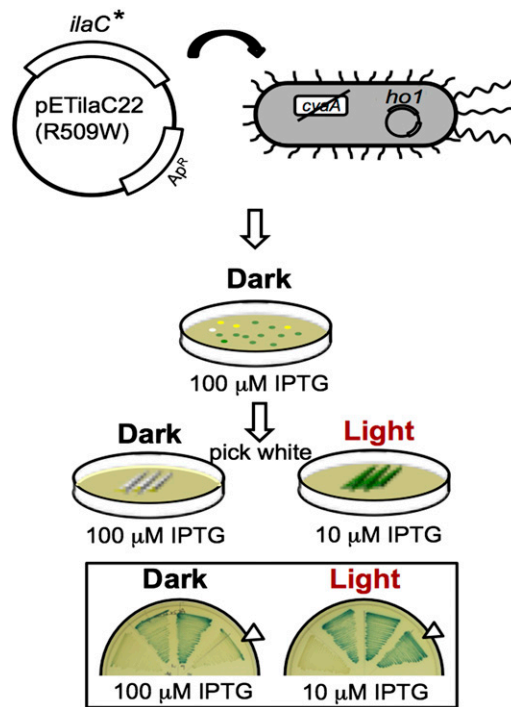


Fig. S2. Selection strategy for isolating IlaC22 R509W mutants with decreased dark AC activities. A library of mutant *IlaC22 R509W* genes was generated by error-prone PCR (mutation frequency of three to four mutations per gene) and cloned in plasmid pET-*IlaC22 R509W* to replace the *IlaC22 R509W* gene. *E. coli* BL21[DE3] *cya* (pT7-*ho1-1*) transformed with the library of mutants was grown at 30 °C, in the dark, on LB plates supplemented with ampicillin (100 μg/mL), kanamycin (50 μg/mL), and IPTG (100 μM). Colonies containing original pET-*IlaC22 R509W* produce blue colonies under these conditions. White colonies were picked and subsequently retested in the presence or absence of light at low (10 μM) and high (100 μM) IPTG concentrations. Irradiation was provided by an All-Red LED grow light panel 225 (30.5 × 30.5 cm; LED Wholesalers). Mutants that produced white colonies in the dark at 100 μM IPTG but blue colonies in the light at 10 μM IPTG were analyzed further. This screen led to identification of the triple mutant, IlaC22 k27 (arrowheads in *Bottom* section).

```

MARGCLMTISGGTFDPSICEMEPATPGAIQPHGALMTARADSGRVAHASVNLGEILGLPAASVLGAPIGEVIGRVN
EILLREARRSGSETPETIGSFRRSDGQLLHLHAFQSGDYMCCLDIEFVRDEDGRLPPGARQSVIETFSSAMTQVELCE
LAVHGLQLVMGYDRVMAYRFGADGHGEVIAERRRQDLEPYLGLHYFASDIPQIARALYLRQVRGAIADACYRFPVLL
GHPELDDGKPLDLTHSSLSRSVSPVHLDYMQNMNTAASLTIGLADGDRWMLVCHNTTPRIAGPEWRAAAGMIGQVV
SLLLSRLGEVENAAETLARQSTLSTLVERLSTGDTLAAAFVAADQLILDVVGASAADVRLAGHELHFGRTPPVDAMQ
KVLDSLGRPSPLEVLSLDDVTLRHPELPELLAAGSGIILLPLTSGDGLIAWFRPEHVQTIITWGGNPAEHGTWNPAT
QRMRPASFDAWKETVTVGRSLPWTSAERNCARELGEAIAAEMAQRTWERKEVTVLFSDIRGYTTLTENLGAAEVVSL
LNQYFETMVEAVFNIEGTLDFIGDALMAVFGAPLPLTENHAWQAVRSALDMRQRLKEFNQRRIIQAQPQIKIGIGI
SSGEVVSNGNIGSHKRMIDYTVIGDGNLSSRLETVTKEYGCDIILSEFTYQLCSDRIRVRQLDKIRVKGKHQAVNIYE
LISDRSTPLDDNTQEFLFHYHNGRTAYLVRDFTQAIACFNSAKHIRPTDQAVNIHLERAYNYQQTTPPPQWDGVWTI
FTKHHHHHH 779

```

Fig. S3. Protein sequences of IlaC22 k27. Four mutations distinguishing IlaC22 k27 from IlaC22 are highlighted in yellow (R209W) and cyan. Y259 mutated in IlaC22 k27 Y259F is highlighted in pink. The sequence derived from BphG is shown in brown; the sequence derived from CyaB1 is shown in green, the C-terminal His₆-tag is shown in black.

```

BphG -----maRGclmtiSGCT-----
PhyB msvgvgvsggggrgggrggeeepssstpnrrRGgeqacSSTKslrprsnstemskaigqytvdarlhavfeq

BphG -----FdpSICG-----MepIatpGaiQPhCaLMtaradSgRVahaSVNlgEILGL---
PhyB sgesgksfdysqslktttYgsSVcEqqitayLsrIqrgCYIQPfcMIavdesSfRIigySseNarEMLGIMPq

BphG -----PaasVLGapIgeVigrvNeILLreArrSgsetp-etIgsfrRSdGllh--LHafqsgdyMcLDdE
PhyB svptlekEeilaLAcdvrsLftssSSILLerAfvAreiIlInpVwihsKNTcKpfaiLHridvc--VVIDdE

BphG FVRQEDgrIppgarqsviEtfsSAMTCVE-----LCElaVhgLQlVlGYDRVmaYRfgaDgHGEVIAEr
PhyB PArtEDpaIasiagavqsgKlavrAISQLCalpggdikLlCDtvvesVRdlTGyDRVMvYKfheDeHGEVIAEr

BphG RRQDLLEPYHGLHYPAASDIPQIAraLYLlRcRVgaHaDacyrFVbLLghpeIddgKpldLthSSDRsvspvHldY
PhyB KRdDLEPYHGLHYPATDIPQASRfLFkQrRVrmIvDcnatPVLVvqddrIt--QsMclvgSTLRaphgdfscY

BphG MgNMnTaASLtlIgL-----aDGD-----RLWGLVCHNTTeIagiapewPaAagmIgeVvsEILS---R
PhyB MaNVGsiASLAmaviingnedDGNvasgrssmRLWGLVCHNTTeSscipfplRyacefLmcafgqLmmeIQ

BphG LgeveNaaetIarCStIstLveRlStgdtlaAafVaadqllDLVgasaFvvrlaQelhfertIpvdaMQkV
PhyB LalqmSekrvIrtQTLlLcdMLLRSS----pagIvtqspSIIDLvKcdGaflyhSKyypIvasevqIKGV

BphG LdsIgrpSplEvlsIddvTLrhpelFellAaCsgIillLpLts-gdgLlaWFRbehvQtlTWGnpaehgtwn
PhyB VEWL-lanHadstgIstgSLgdagyFgaalGdaVcgmAvaYitkrEflWFRshstakeIkWGG-akhIpedk

BphG patQRMRFRASfdaWkdvvtorsIIPwtSAE-----fNcaRElgeAiaAEMaqrt
PhyB ddgQRMRFRSSfdaWkdvvtorsIIPwtSAE-----mdaihsIqlilRsfKfseaAMnSKVvdgv

R250A Y259F
R582A
G450E

```

Fig. S4. Identification of residues involved in slowing the dark thermal recovery of IlaC. Shown is alignment of the *Rhodobacter sphaeroides* BphG bacteriophytochrome and the *Arabidopsis thaliana* phytochrome PhyB. Residues of PhyB affecting its photocycle and conserved in BphG are highlighted in yellow. Mutations of PhyB that extend the lit far-red-absorbing state of PhyB are shown in red.

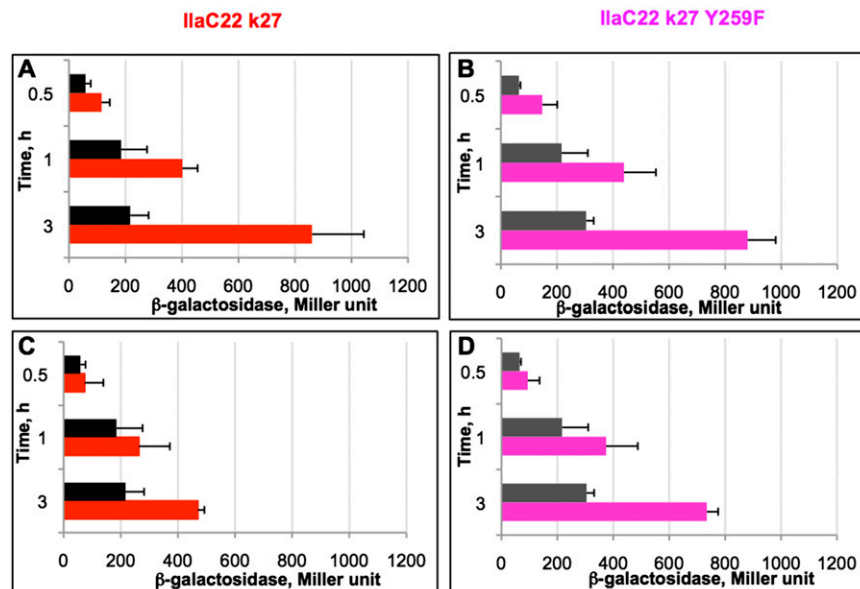


Fig. S5. Effects of IlaC k27 and IlaC k27 Y259F on cAMP-CRP-dependent *lacZ* gene expression in *E. coli*. Strain BL21[DE3] *cya* (pT7-ho1-1) containing either pET-ilaCK27 or pET-ilaC k27 Y259F were grown in culture tubes on a shaking platform at 30 °C in LB supplemented with ampicillin (50 µg/mL) and kanamycin (50 µg/mL). When optical densities of the cultures reached A_{600} 1.5, IPTG (1 mM, final concentration) was added to induce *ilaC* gene expression. Irradiation was provided to by an All-Red LED grow light panel. Tubes containing “dark” samples were wrapped in aluminum foil to avoid light exposure. Samples were withdrawn at the indicated time points (0.5, 1, and 3 h) postinduction for determination of β -galactosidase activities, which was measured by the Miller method (1). (A), IlaC k27; (B), IlaC k27 Y259F. (A and B) Constant irradiation; (C and D) pulsed irradiation (30 s light, 90 s dark). Black or dark-gray bars, dark; red or pink bars, light. Error bars show SD derived from three independent experiments.

1. Sambrook J, Fritsch EF, Maniatis T (1989) *Molecular Cloning: A Laboratory Manual* (Cold Spring Harbor Lab Press, Cold Spring Harbor, NY), 2nd Ed.



Movie S1. Red light stimulated locomotion of an animal expressing IlaC22 k27 in cholinergic neurons (*Punc-17:ilaC*, strain: NQ721). The animal is exposed to green light for 10 s followed by red light for 10 s. The transgenic animal can be seen speeding up upon exposure to red light and performs more body bends over the same time period.

[Movie S1](#)